Langmuir
Article
pubs.acs.org/Langmuir

Controlled Flats on Spherical Polymer Colloids

Laura Mely Ramírez,[†] Scott T. Milner,[†] Charles E. Snyder,[†] Ralph H. Colby,*[,‡] and Darrell Velegol*[,†]

[†]*Department of Chemical Engineering and* [‡]*Department of Materials Science and Engineering, The Pennsylvania State University, University Park, Pennsylvania 16802*

Received November 2, 2009. Revised Manuscript Received December 13, 2009

Colloidal particles with heterogeneous surfaces offer rich possibilities for controlled self-assembly. We have developed a method for preparing micrometer-sized polystyrene spheres with circular flat spots of controlled radius and location. The flats are created by settling the particles onto a flat glass substrate and then raising the temperature above the glass-transition temperature of the polymer for a controlled time (t). The polymer particle spreads on the glass such that the radius of the flat grows with time. We present a scaling theory for the hydrodynamics of the flattening process, finding that the radius of the flat grows as $t^{1/3}$. The model is in good agreement with our experimental observations of the flat radius versus spreading time as well as with previous studies in the literature for sintering polymer spheres.

Introduction

Considerable research has gone into fabricating patchy particles in which the patch is chemically different from the rest of the particle. Particle patches have included electrostatic charge,[1] polymer,[2] gold,[3,4] and even targeting ligands.[5] However, seldom has the patch consisted of a small geometric or physical deformation.[6] In this article, we describe a simple experimental method for creating a flat region on a polymer colloid, and we provide guidance for controlling the size of the patch on the basis of a scaling model that we have developed. We hypothesize that such micrometer-sized flattened spheres will preferentially aggregate flat face to flat face under depletion forces, leading to "colloidal dimers" and eventually "colloidal polymers" with two flat regions on each particle. These colloidal chains are expected to provide insight into current polymer systems that have limited testing as a result of characteristic small sizes and rapid time scales.

Our method for creating flats consists of four main steps: (1) electrostatically adhering particles to a flat surface; (2) heating the sample to above the glass-transition temperature (T_g) of the polymer to allow particle deformation by spreading; (3) cooling the particles back to below their T_g; and (4) sonicating the particles off the substrate to obtain spherical polymer colloids that have a flattened patch. We are able to measure the radius (s) of the flattened regions (i.e., "flats") after any given spreading time (t).

The flat grows because of spreading caused by surface tension forces. One well-known model for describing the spreading of a droplet due to surface tension is Tanner's law.[7,8] This model predicts that the radius of the spread droplet grows as $s \sim t^{1/10}$, and the model is well supported by experimental data. However, Tanner's law applies to liquids that fully wet the surface (zero contact angle) such that an analysis enables one to use lubrication hydrodynamics near the contact line.[9] In our case, the polymer colloids turn out to have equilibrium contact angles of greater than 90°. Furthermore, Tanner's law does not hold at early times, whether or not the droplet wets the surface, and we are interested in early times. Thus, the assumptions inherent in Tanner's law do not apply even with the modifications that have appeared in the literature for fluids that do not perfectly wet surfaces.[10−14]

A more closely related problem to ours is sintering. Sintering is the coalescence of two or more particles under the action of capillary forces.[15] Powder metallurgy, ceramics, polymer powder, rotational molding, and fluidized-bed coating are important industrial processes that rely on sintering.[16,17] For instance, rotational molding, also known as "rotomolding", is one of the fastest growing segments of the plastics industry. Rotomolding has many advantages over other plastics processing methods.[18] It is used to fabricate tanks ranging from 0.019 to 88 m^3 in volume as chemical, agricultural, and recreational vehicles. Playground equipment, toys, portable toilets, battery cases, garbage containers, and other products are also produced by rotational molding. Polymers such as polyethylenes have been the principal material used as resins because of their excellent flexibility, ease of molding, uniform shrinkage, and low cost. Controlling the sintering process of polymer particles is essential to achieving a reliable rotomolding method.

Frenkel was the first to model the hydrodynamics of the early stages of sintering. In his model, he balanced the work due to both the viscous dissipation and the surface tension (i.e., the reduction

*To whom correspondence should be addressed. Phone: (814) 865-8739. Fax: (814) 865-7846. E-mail: rhc@plmsc.psu.edu; velegol@psu.edu.

(1) Chaturvedi, N.; Jerri, H.; Velegol, D. *Langmuir* **2008**, *24*, 7618.
(2) Pawar, A. B.; Kretzschmar, I. *Langmuir* **2008**, *24*, 355.
(3) Zhang, G.; Wang, D.; Mohwald, H. *Nano Lett.* **2005**, *5*, 143.
(4) Zhang, G.; Wang, D.; Mohwald, H. *Angew. Chem., Int. Ed.* **2005**, *44*, 1.
(5) Yake, A. M.; Zahr, A. S.; Jerri, H. A.; Pishko, M. V.; Velegol, D. *Biomacromolecules* **2007**, *8*, 1958.
(6) Chaudhury, M. K.; Whitesides, G. M. *Langmuir* **1991**, *7*, 1013.
(7) Tanner, L. H. *J. Phys. D: Appl. Phys.* **1979**, *12*, 1473.
(8) Bonn, D.; Eggers, J.; Indekeu, J.; Meunier, J.; Rolley, E. *Rev. Mod. Phys.* **2009**, *81*, 739.
(9) Leger, L.; Joanny, J. F. *Rep. Prog. Phys.* **1992**, *55*, 431.
(10) Tanner, L. H. *J. Phys. D: Appl. Phys.* **1986**, *19*, 751.
(11) McHale, G.; Rowan, S. M.; Newton, M. I. *J. Phys. D: Appl. Phys.* **1994**, *27*, 2619.
(12) de Gennes, P. G. *Rev. Mod. Phys.* **1985**, *57*, 827.
(13) Seaver, A. E.; Berg, J. C. *J. Appl. Polym. Sci.* **1994**, *52*, 431.
(14) Alteraifi, A. M.; Sherif, D.; Moet, A. *J. Colloid Interface Sci.* **2003**, *264*, 221.
(15) Kingery, W. D.; Bowen, H. K.; Uhlmann, D. R. *Introduction to Ceramics*, 2nd ed.; John Wiley & Sons: New York, 1976.
(16) Crawford, R. J. *Rotational Moulding of Plastics*; John Wiley & Sons: New York, 1992.
(17) Jagota, A.; Dawson, P. R. *Acta Metal.* **1988**, *36*, 2551.
(18) Mark, H. F. *Encyclopedia of Polymer Science and Technology*; John Wiley & Sons, Inc.: New York, 2004; Vol. *11*.

in interfacial energy).[19] Frenkel's model predicts that the radius of the flat scales as $s \sim t^{1/2}$. Many scientists have modified and/or corrected Frenkel's model, in part because of known errors in the original derivation. Nevertheless, most researchers have maintained his $t^{1/2}$ scaling.[20,21]

Our objectives in this work were (1) to create patchy particles consisting of a flat region on a spherical colloid and (2) to model the size of the flat as a function of spreading time to gain better control over the process. As we conducted our flattening process described above, we took data for how the radius (s) of the flat changed with spreading time (t). The data do not indicate the $t^{1/2}$ scaling found by Frenkel and later researchers.

We re-examined the hydrodynamics of sintering and derived a scaling model that shows that at early times the radius of the flat (s) scales as $t^{1/3}$. The important results from this work are (1) a simple method for creating flats on polymer colloids, (2) data for the spreading rate of a micrometer-sized polymer particle above its T_g on a solid flat surface, and (3) a scaling model that accurately predicts the size of the flat as a function of spreading time.

Experimental Section

Materials. The polymer particles to be flattened were monodisperse, surfactant-free, amidine-functionalized polystyrene latex (PSL) microspheres (average molecular weight, 70 000 g/mol; average diameter, 3.3 μm; coefficient of variation, 8.7%; batch no., 1414,1), purchased from Interfacial Dynamics Corporation (Portland, OR). The Pyrex glass Petri dishes (diameter, 7.0 cm) used as flat substrates were obtained from VWR International. Silicon wafers, with an orientation of ⟨1-0-0⟩ and resistivity values of 1−10 Ω·cm, were used as substrates for field-emission scanning electron microscopy (FESEM) imaging and as v-groove template substrates. The silicon wafers were purchased from Silicon Quest International (lot no: IMV3P01-10PRM). Deionized (DI) water from a Millipore Corporation Milli-Q system with a specific resistance greater than 1 MΩ·cm was used for all experiments.

Instrumentation. The pressurized heat treatments to flatten the particles were carried out in a Consolidated Stills & Sterilizers steam autoclave (model Steromaster MKII) at 120 °C and 18 psig. An ultrasonicator from VWR International (model 550T) was used to remove the particles from the flat substrates. The optical microscopy images were taken using a 20× magnifying lens on a Nikon Eclipse TE2000-U inverted optical microscope.

FESEM Sample Preparation. A ZeissSMT 1530 field-emission scanning electron microscope (FESEM) at the Penn State Nanofabrication Facility was used to acquire the electron microscopy images and length measurements. Flattened particles in solution (2.0 μL, <0.01% solids) were pipetted onto a small silicon wafer and left overnight to air dry in a dust-free laminar-flow hood. FESEM images were taken at a working distance of 3 to 4 mm and a gun power of 0.5−1 kV.

Particle Flattening Technique. Conditions that give well-formed flat regions on polymer particles were found. Because of electrostatic forces in the aqueous solutions, positively charged particles in water adhere to negatively charged glass surfaces. Piranha-etched Petri dishes were used as the flat glass substrates. After the cationic amidine polystyrene particles were electrostatically adhered to the anionic Petri dish, the Petri dish was imaged using an optical microscope (Figure 1a). The adhered particles were copiously washed with DI water to remove any nonadhered particles free in solution. Our experiments showed that the rinsing step removed very few adhered particles from the flat substrate.

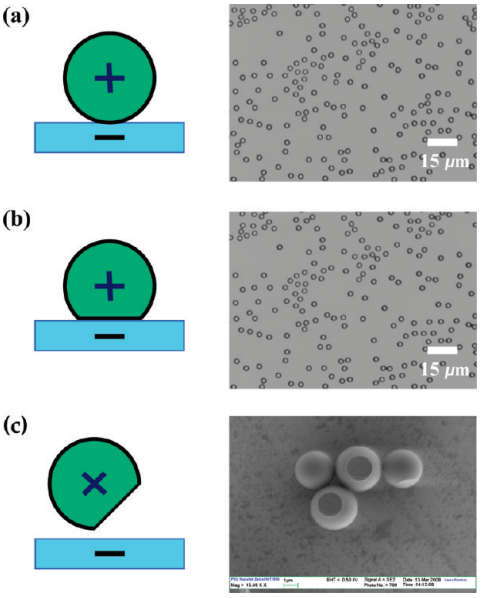

Figure 1. Polystyrene microspheres flattened in one spot. (a) Positively charged 3.3 μm amidine-functionalized PSL particles in DI water were electrostatically adhered to a negatively charged flat glass substrate. Shown is an optical microscopy image (20× air objective) of 3.3 μm amidine-functionalized PSL particles adhered to a flat glass Petri dish. (b) The sample was placed in a standard heat autoclave (120 °C, 18 psig) to flatten particles in one spot. Shown is an optical microscopy image (20× air objective) of flattened 3.3 μm amidine-functionalized PSL particles electrostatically adhered to a flat glass Petri dish after rinsing with DI water several times. Note that very few particles were removed from the substrate. (c) The particles were sonicated off the surface to obtain single flattened microsphere colloids in water. An FESEM image is shown for flattened 3.3 μm amidine-functionalized PSL particles. The FESEM image had a gun power of 0.5 kV, a working distance of 4 mm, and a magnification of 15 490×.

At this point, the particles were ready to be flattened. Spherical particles were flattened in an autoclave (120 °C, 18 psig) above their glass-transition temperature (T_g = 100 °C for polystyrene)[22] without evaporating the solvent. Being slightly above T_g, the particles deformed primarily because of surface tension, spreading onto the flat surface (Figure 1b). Gravity played a negligible role in the flattening because of the small size of the particles. After several minutes, the samples were taken from the autoclave and again rinsed with DI water numerous times to ensure that only the flattened particles remained in the final step. The flattened particles, still electrostatically adhered to the flat glass Petri dish after heat treatment but now cooled to room temperature, were imaged using an optical microscope (Figure 1b). Finally, the samples were placed in an ultrasonicator for 2 min to remove the majority of the particles from the flat substrate. An FESEM was then used to image the single flattened particles (Figure 1c). The flattened particles in water can also be induced to form dimers by adding either salt or polymer (depletion flocculation), and this shall be the subject of a future publication.

Note that for the adhesion step a surface coverage fraction (ϕ_s) of approximately 10% was used, as seen in Figure 1a. When submonolayer coverage is used, single flattened spherical particles are formed (Figure 1c). Thus, using the particle-flattening technique described in Figure 1, about 5×10^7 particles with a flattened patch can be obtained for one sample if, for instance, 3 μm particles are settled onto a 7.0 cm Petri dish with $\phi_s = 0.10$. The precise coverage is not important as long as particles do not form more than a single layer or even become so dense on

(19) Frenkel, Y. *J. Phys.* (*Paris*) **1945**, *9*, 385.
(20) Pokluda, O.; Bellehumeur, C. T.; Vlachopoulos, J. *AIChE J.* **1997**, *43*, 3253.
(21) Bellehumeur, C. T.; Kontopoulou, M.; Vlachopoulos, J. *Rheol. Acta* **1998**, *37*, 270.
(22) Wünsch, J. R. *Polystyrene Synthesis, Production, and Applications*; Rapra Technology Ltd.: U.K., 2000; Vol. *10*, No. 4.

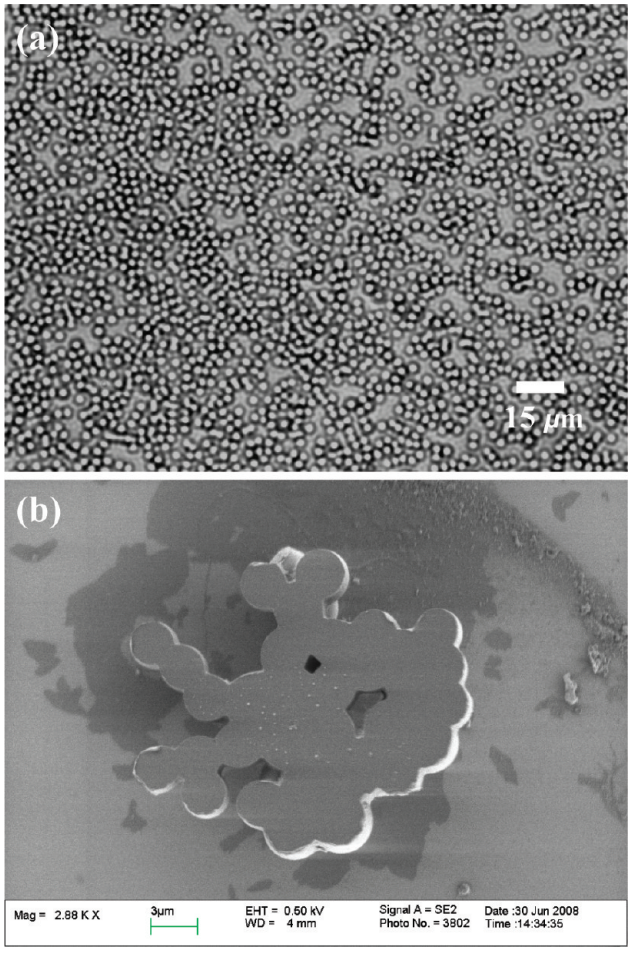

Figure 2. Particles fusing together when the surface coverage is too high. Cationic particles were adhered to a flat glass surface and flattened for 4 h in an autoclave (120 °C, 18 psig). (a) Optical microscopy image (20× air objective) of 3.3 μm amidine-functionalized PSL particles ($\phi_s \approx 0.70$) electrostatically adhered to a flat glass Petri dish. (b) FESEM image of flattened 3.3 μm amidine-functionalized PSL particles fused together, having formed a cluster. The FESEM image had a gun power of 0.5 kV, a working distance of 4 mm, and a magnification of 2880×.

the surface that particle clusters form as the particles spread (Figure 2). We have kept $\phi_s < 0.15$ to avoid particle clusters.

Modeling

In this section, we describe our model in the early stages of the spreading of a polymer particle on a surface. The particle is above its T_g, so we proceed in a manner similar to how one models the sintering of two identical viscous spherical particles, with the value of the interfacial tension appropriately replaced. The spherical cap geometry applies (Figure 3).

We model the particles as a viscous Newtonian fluid because the longest relaxation time for the polystyrene microspheres is much less than the typical flattening time in our experiments. The longest relaxation time of 500 s for the polystyrene chains is estimated by dividing the viscosity of polystyrene at the flattening temperature (roughly 100 MPa·s at 120 °C, estimated using the WLF equation) by its plateau modulus (0.2 MPa).[23] This allows us to ignore viscoelastic effects. The viscous effects from the surrounding fluid are also ignored because the viscosity of the

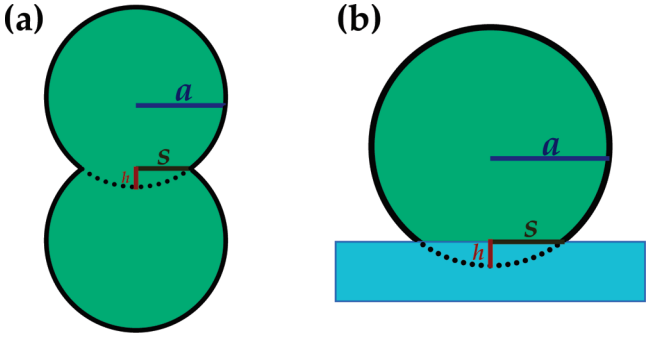

Figure 3. Schematic of particle deformation in the early stages. The particle radius (a), the contact radius (s), and the particle displacement beyond a contact distance (h) are geometrically related. (a) Two equally sized spheres merging into each other in the early stages. (b) Particle settled onto a flat substrate during the flattening process in the early stages. By symmetry, the modeling of the sphere−sphere interaction is the same as that of the sphere−flat interaction in the early stages.

polymer particle is much greater than that of the surrounding medium.

We approximate that the particle radius (a) remains constant for two equally sized spheres merging during the early stages. The original particle shape will change as the spreading proceeds in order to conserve the volume of the system, but the change is very slight in the early stages of the flattening process. Thus, the parameters displayed in Figure 3 have the following scaling relationship by a parabolic approximation:

$$s^2 \sim ha \tag{1}$$

The reduction of interfacial energy W is the origin of the attractive force F as the particles merge. We have

$$W \sim \gamma s^2 \tag{2}$$

where γ is the interfacial energy change per unit area, accounting for the polymer−glass, water−glass, and polymer−water interfacial tension.[24] The corresponding attractive force is given by the derivative of this energy with respect to the displacement of the sphere,

$$F \sim \frac{\partial W}{\partial h} \sim \gamma a \tag{3}$$

The resulting force F is constant, independent of particle displacement. As the particles approach each other, the rate of work done by the attractive force F is

$$\dot{W} \sim F\dot{h} \tag{4}$$

This must balance the rate of viscous dissipation within the particle,

$$\dot{W} \sim \eta\dot{\varepsilon}^2\Omega \tag{5}$$

where η is the particle viscosity, $\dot{\varepsilon}$ is the typical strain rate, and Ω is the dissipation volume.

This balancing of the work and dissipation is the same approach that Frenkel used. However, our estimate of the

(23) Colby, R. H.; Rubinstein, M. *Polymer Physics*; Oxford University Press: New York, 2003.

(24) Adamson, A. W. *Physical Chemistry of Surfaces*, 5th ed.; John Wiley & Sons: New York, 1990; p 385.

magnitude of the dissipation differs from his. (See below.) The key point is to assess properly the magnitude of the flow gradients as well as the volume of the region over which the flow is appreciable. We assert that the gradients of the Stokes flow are arguably on the order of $1/s$ and that the volume is on the order of s^3, anticipating the spatial dependence of a field satisfying a Laplace equation. The strain rate is then $1/s$ times a typical velocity in the flow field, which ought to be $\dot{h}$, hence

$$\dot{\varepsilon} \sim \dot{h}/s \tag{6}$$

Combining these results, we find

$$s(t) \sim \left(\frac{Fat}{\eta}\right)^{1/3} \tag{7}$$

Our scaling result for sintering flow is strongly analogous to the description of a Hertzian elastic contact in which the contact radius scales as $(Fa/G)^{1/3}$, where G is the shear modulus.[25] Using the scaling for the attractive force, from eq 3, we have

$$\frac{s(t)}{a} \sim \left(\frac{t\gamma}{\eta a}\right)^{1/3} \tag{8}$$

where γ/η is defined as the "sintering rate". Equation 8 is the key modeling result in this article, giving the scaling for the spreading radius (s) of the flat as a function of time and also as a function of other pertinent variables in the system. In fact, a precise calculation of the flow field in the early stages of sintering can be given, by close analogy to the treatment of a Hertzian contact.[26,27] The result,[27] completely consistent with our scaling arguments, is

$$\frac{s(t)}{a} = \left(\frac{3\pi t\gamma}{32\eta a}\right)^{1/3} \approx 0.665\left(\frac{t\gamma}{\eta a}\right)^{1/3} \tag{9}$$

Note that the scaling from eq 8 does not agree with Frenkel's model, which is

$$\frac{s(t)}{a} \sim \left(\frac{t\gamma}{\eta a}\right)^{1/2} \tag{10}$$

However, Frenkel's result is based on faulty scaling assumptions, namely, $\dot{\varepsilon} \sim \dot{h}/a$ and $\Omega \sim a^3$. In other words, the characteristic length scale for gradients was incorrectly taken by Frenkel to be a, not s. Equations 8−10 introduce a natural time scale $\eta a/\gamma$ for sintering and flattening that we will make use of later.

Results and Discussion

Using our particle-flattening technique, experiments were run to investigate how the flat size changes with spreading times (Figure 4). The radius (s) consistently increased with increasing time. To confirm the qualitative results, length measurements were taken for images captured for many particle samples.

Examining the data for the flat size (s) as a function of time (t) from the experiments shown in Figure 4 led us to develop our scaling model, described earlier. We tested our scaling model with

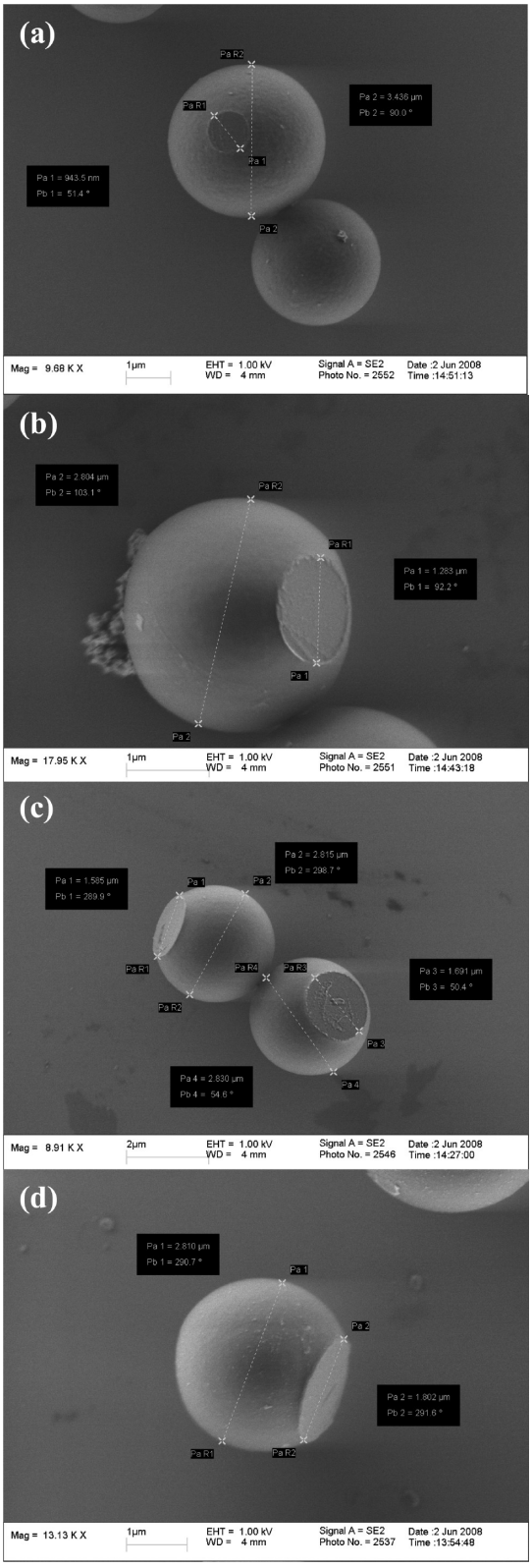

Figure 4. Flattened regions on polymer particles. FESEM images of 3.3 μm amidine-functionalized PSL particles settled in DI water and placed in the autoclave at 120 °C and 18 psig for (a) 15, (b) 30, (c) 45, and (d) 60 min. The radius measurements of the flat region and the particle were taken with a software tool embedded in the FESEM imaging program. The FESEM images had a gun power of 1 kV, a working distance of 4 mm, and magnifications of (a) 9680×, (b) 17 950×, (c) 8910×, and (d) 13 130×.

(25) Hertz, H. *Miscellaneous Papers*; Jones, D. E., Schott, G. A., Translators; Macmillan and Co.: London, 1896.
(26) Landau, L. D.; Lifshitz, E. M. *Theory of Elasticity*, 3rd ed.; Sykes, J. B., Reid, W. H., Translators; Course of Theoretical Physics; Reed Educational and Professional Publishing: Oxford, U.K., 1986; Vol. 7.
(27) Milner, S. T. Hydrodynamics of Sintering at Early Times. To be submitted for publication, **2010**.

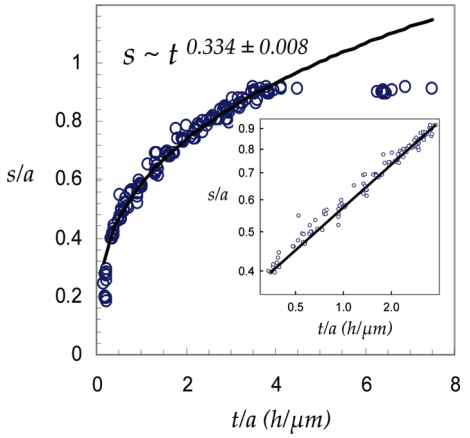

Figure 5. Flat size as a function of time. All circles are open (○), although many of them overlap because we took 10 data points per time point. The dimensionless contact radius (s/a) of amidine-functionalized PSL particles is plotted as a function of time (t/a in h/μm) for 0.25−10 h. The actual time has an uncertainty of about 2 min because of variations in handling the materials as they go into and out of the autoclave. The radius has an uncertainty of about 30 nm, found from the FESEM measurements. Note that there is a plateau region at later times, beyond 6 h, suggesting an equilibrium contact angle. The inset image displays s/a versus t/a (h/μm) on a log−log scale for 0.5−5.5 h. The exponent for the time dependence of the flat radius is 0.334, with a 95% confidence interval of 0.008. Because of the polydispersity of the particle sample, s/a is plotted as a function of t/a to account for the particle radius dependence in eq 8.

the data from the early stages of flattening. The spreading times were varied from 0.25 to 10 h. Figure 5 shows the dimensionless contact radius (s/a) plotted as a function of time (t/a).

The data taken at 15 min = 900 s did not match our predictions. Of course, at such early times, viscoelastic stresses are likely important because this time is only a factor of 2 larger than our estimate (detailed earlier) of the longest polymer relaxation time of 500 s and the thermal equilibrium time, estimated to be 2 min, is not negligible for the 15 min data. At much longer times, beyond roughly 6 h, we found that an equilibrium contact angle was reached. At 5.5 h of spreading, the particles had a flat diameter that was approximately 90% of the original particle diameter, which was statistically the same as that for 6 h and also for 10 h. Hence, we see an exponential approach to equilibrium with the time scale being proportional to the sintering rate. (See the plateau region in Figure 5).

Following our scaling relationship, we fit our data to the following model:

$$s \sim t^n \tag{11}$$

In fitting our data, we ignored the 15 min time, which likely has viscoelastic behavior. The 6−10 h times, which are close to equilibrium, were ignored as well because the physics of reaching equilibrium is not included in our scaling model. We thus use data from 0.5 to 5.5 h and do a power fit to the experimental values. Our fit for the exponent is $n = 0.334 \pm 0.008$, where the uncertainty is calculated to be the 95% confidence interval. The data thus support our $t^{1/3}$ scaling model.

Figure 6 shows a comparison between the present data and experimental data from Pokluda et al. and Bellehumeur et al.[20,28] In the original papers, the data was fit to a power law of $t^{1/2}$;

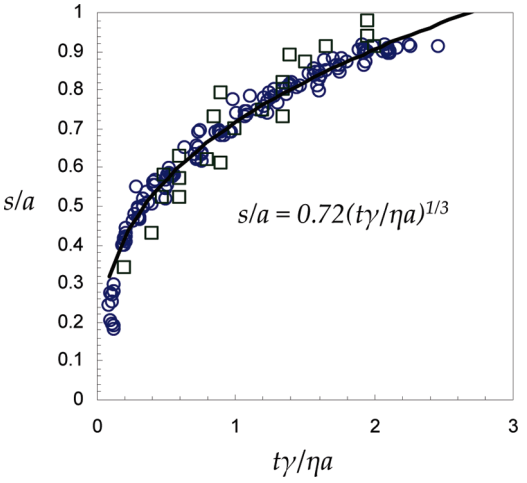

Figure 6. Comparison between present data and experimental data from the literature. The dimensionless contact radius (s/a) is plotted as a function of the dimensionless sintering time ($t\gamma/\eta a$). These experimental data from the literature, represented by open squares (□), were taken using rotomolding-grade high-density and linear low-density polyethylene resins ranging from 330 to 600 μm in diameter at 130 and 170 °C (refs 20 and 28). A sintering rate (γ/η) of 0.54 μm/h was used for our data, open circles (○), in order to match the fit to the data in the literature of $s/a = 0.72(t\gamma/\eta a)^{1/3}$. This sintering rate would be consistent, for example, with $\eta = 100$ MPa·s and $\gamma = 15$ mJ/m^2.[23,29] Both data sets agree fairly well. Deviations from the literature data are partially due to the irregular shape of the resins.

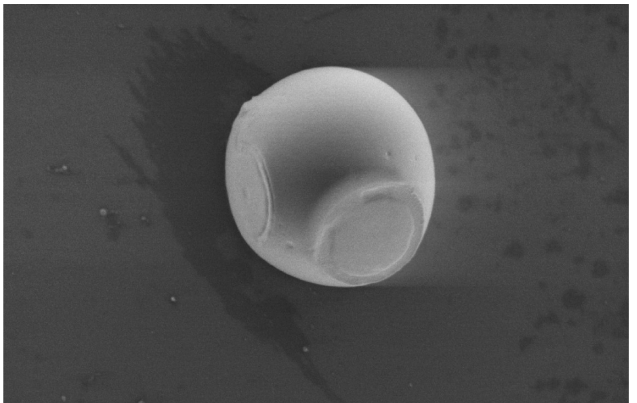

Figure 7. FESEM image of an amidine-functionalized PSL particle with two flattened sides. The particles were settled in DI water onto a nanofabricated v-groove template etched in a silicon wafer. Next, the sample was placed in an autoclave at 120 °C and 18 psig for 90 min. Each flattened side has a radius of 0.84 ± 0.03 μm, and the particle radius is 1.48 ± 0.03 μm. According to our model, if we use the 0.72 fitted prefactor and a sintering rate (γ/η) of 0.54 μm/h, then a 2.96 μm amidine-functionalized PSL particle with a spreading time of 90 min will have a flat radius of 0.87 ± 0.03 μm. The FESEM image had a gun power of 0.5 kV, a working distance of 3.6 mm, and a magnification of 33 860×.

however, our analysis shows that a $t^{1/3}$ power law fits the data much better. Furthermore, because the authors had estimated the interfacial tension and measured the viscosity of their polymer particles at their target sintering temperature, we were able to do a power fit to the prefactor from their data. The time exponent was

(28) Bellehumeur, C. T.; Bisaria, M. K.; Vlachopoulos, J. *Polym. Eng. Sci.* **1996**, *36*, 2198.

(29) Wu, S. *Polymer Interface and Adhesion*; Marcel Dekker: New York, 1982.

fit to 1/3, consistent with our data and our model. It turns out that the 1/3 power law fits the data from refs 20 and 28 better than the 1/2 power law that they used in their own paper. We then used their data, with their estimates of the interfacial tension and measurement of viscosity, to fit the prefactor as 0.72. Of course, the exact value of the prefactor depends upon the accuracy of the γ and η values from the authors. We hypothesize that when the uncertainties in γ and η are included the fitted value of 0.72 is within the statistical uncertainty of the 0.665 prefactor listed in eq 9. Hence, eq 9 is given as a general equation that should be applicable to a range of materials.

The amidine-functionalized polystyrene latex particles are known to hydrolyze upon long periods of heating.[30] The hydrolysis of amidine functional groups at the surface occurs in two reactions: uncharged amide groups form in the first step and carboxyl groups are formed more slowly in the subsequent step.[31] Although amidine hydrolysis would likely affect the interfacial tension of the functionalized polymer particle with the water medium and the glass substrate, the data presented in this article remains consistent with the scaling model.

We ran an additional experiment to examine how spreading occurs if we form two flats on a single particle (Figure 7). To form two flats, we settled the particles onto a nanofabricated v-shaped template in a silicon wafer.[32] The size of both flats on the particle follows our model with the fitted prefactor of 0.72 and an estimated sintering rate of 0.54 μm/h. Such twice-flattened particles and their assembly into polymers will be the subject of a future publication.

Conclusions

By applying our particle-flattening technique, we were able to create patchy particles consisting of a flat region on a spherical colloid. Experimental data shows that our scaling model with a fitted prefactor is able to predict the radius of the flattened region as a function of time. The data and the model as well as previous data in the literature all indicate that the scaling for the flat region's radius is $t^{1/3}$ rather than $t^{1/2}$.

We are currently working to build chain assemblies from our flattened spheres. By adjusting the ionic strength or depletant concentration of the solution, particles with one flattened patch can form doublets whereas particles with two flattened patches can form into polymer chains because of the favorable and stronger energetic interactions for a flat−flat orientation. We hypothesize that the particle chains formed from particles with two flats would be flexible because the particles would reside in a fairly deep DLVO secondary energy minimum, leaving a layer of fluid between the flattened particles and giving freely jointed chains. These "polloidal chains" are expected to enable additional fundamental studies of polymer systems because of their ready visibility in an optical microscope and their much slower dynamics.

Acknowledgment. We thank the National Science Foundation (CBET grant no. 0730780) for funding this project and the Penn State Nanofabrication Facility for FESEM imaging equipment and v-groove template fabrication. Stephen Garoff is thanked for his valuable discussions and insights on Tanner's law.

Supporting Information Available: Microscopy videos of 3.3 μm amidine-functionalized PSL particles undergoing Brownian motion in solution were captured with a 100× oil objective to observe the key difference in geometry between a spherical colloid and a spherical particle with a flat patch. Note that the microsphere is completely symmetric whereas the patchy particle, with a darker spot corresponding to its flat region, is asymmetrical. This material is available free of charge via the Internet at http://pubs.acs.org.

(30) Kolthoff, I. M.; Miller, I. K. *J. Am. Chem. Soc.* **1951**, *73*, 3055.
(31) Seebergh, J. E.; Berg, J. C. *Colloids Surf., A* **1995**, *100*, 139.
(32) Madou, M. J. *Fundamentals of Microfabrication: The Science of Miniaturization*, 2nd ed.; CRC Press: New York, 2002.